


History-dependent nonequilibrium conformations of a highly confined polymer globule in a sphere

Seulki Kwon and Bong June Sung

Department of Chemistry, Sogang University, Seoul 121-742, Republic of Korea (Received 20 April 2020; accepted 28 July 2020; published 20 August 2020)

Chromatin undergoes condensation-decondensation processes repeatedly during its cell lifetime. The spatial organization of chromatin in nucleus resembles the fractal globule, of which structure significantly differs from an equilibrium polymer globule. There have been efforts to develop a polymer globule model to describe the fractal globulelike structure of tightly packed chromatin in nucleus. However, the transition pathway of a polymer toward a globular state has been often ignored. Because biological systems are intrinsically in nonequilibrium states, the transition pathway that the chromatin would take before reaching the densely packaged globule should be of importance. In this study, by employing a simple polymer model and Langevin dynamics simulations, we investigate the conformational transition of a single polymer from a swollen coil to a compact globule. We aim to elucidate the effect of transition pathways on the final globular structure. We show that a fast collapse induces a nonequilibrium structure even without a specific intramolecular interaction and that its relaxation toward an equilibrium globule is extremely slow. Due to a strong confinement, the fractal globule never relaxes into an equilibrium state during our simulations such that the globular structure becomes dependent on the transition pathway.

DOI: [10.1103/PhysRevE.102.022501](https://doi.org/10.1103/PhysRevE.102.022501)**I. INTRODUCTION**

The condensation-decondensation process of chromatin inside cell nucleus leads to various chromatin structures, which relates closely to its functions such as gene regulation [1,2]. Understanding the chromatin structures inside a nucleus should be, therefore, a topic of interest. The spatial organization of chromatin in cell nucleus differs significantly from what is expected for an equilibrium polymer globule [3]. There have been great efforts to develop a polymer model and describe the out-of-equilibrium chromatin structure [4–11]. Most studies, however, focused on the globular state, while the pathway for the condensation of a chromatin fiber has been often ignored. Because biological systems may stay in nonequilibrium states and the chromatin conformation in nonequilibrium states may fluctuate significantly, the transition pathway might affect the conformation of densely packed globule, especially when the conformational relaxation of the chromatin slows inside a confined space. The purpose of this study is to elucidate the effect of a transition pathway on the conformation of a polymer globule, which could provide physical insight on the nonequilibrium conformations of chromatin beyond biological details.

Recent advances in single-cell imaging and chromosome capture methods [12,13] revealed that the chromatin conformation inside nucleus was totally different from equilibrium conformations. Genome-wide 3C (Hi-C) experiments [3] provided information on chromatin conformations by measuring the probability of a contact $P(s)$ between two loci separated by a genomic distance s . If the chromatin were to behave like an equilibrium polymer globule [14], it would have highly entangled conformations with many knots and would behave like a random walk chain. $P(s)$ should scale as $P(s) \sim s^{-3/2}$,

which can be obtained from the ideal chain statistics with the flory exponent $\nu = \frac{1}{2}$. However, Lieberman-Aiden *et al.* [3] reported that the contact probability [$P(s)$] of human chromosomes exhibited $P(s) \sim s^{-1.08}$ at a megabase scale. The scaling exponent of -1 is consistent with that of a crumpled globule, which is a metastable polymer globule that forms through the collapse of polymer local segments. It is also known as the *fractal* globule and its scaling relation, i.e., $P(s) \sim s^{-1}$, was estimated by a space-filling Peano curve [15]. This indicates that the human chromosomes at megabase scales have fractal globulelike structures without knots. In addition, the structure of chromosomes is different in different organisms and cell types [3,8,13,16,17]. Such different structures far away from equilibrium polymer globules may relate to the presence of chromosome territories [18,19], of which physical origin remains unclear.

In order to prepare and investigate the fractal globules as a model for chromatin conformations, polymer models were developed by incorporating specific interactions into the Hamiltonian of the polymer. Binder-mediated interactions [9] or randomly formed dynamic loops [6,20] could make polymers to have a fractal globule structures as free-energy minimum (i.e., equilibrium) conformations. However, such models with specific interactions do not allow one to investigate the effect of the transition pathway along nonequilibrium states on the globule structure. Previous experiments (including Hi-C and fluorescent *in situ* hybridization experiments) showed unexpected cell-to-cell variability in isogenic samples, which indicates that the chromatin would be in nonequilibrium states instead of the free-energy minimum state. Moreover, recent simulations [21] showed that a highly confined polymer, as a model for chromosome in cell nucleus, exhibited glassy dynamics as the polymer packing fraction increased.

In this study, we aim to elucidate the nonequilibrium nature of the transition pathway and its effect on the conformational transition. There have been extensive evidences that biological and polymeric systems would stay in nonequilibrium states [22–33]. Equilibrium thermodynamics presumes that a transition from one to another state would follow a reversible pathway, along which every single state should be in local equilibrium. In many biological systems, however, such presumption may not hold, as reported for enzymatic kinetics [24,26], protein folding [27], transport in membranes [25], and viral DNA packaging [28,34].

We perform molecular simulations and investigate the conformational transition of a single polymer chain from a coil to a globule. A spatial confinement forces the polymer to have a globular conformation. Chromatin is confined in a cell nucleus, of which size varies depending on the cell types, the stage of development, and protein contents [35,36]. Significant changes in available space for chromatin could induce chromatin folding. If a densely packed polymer exhibits nonequilibrium dynamics and the polymer conformation hardly relaxes into its equilibrium conformation, the polymer conformation would be determined by the transition pathway it takes rather than equilibrium thermodynamics. We employ a flexible bead-spring polymer chain with no specific interactions between monomers in order to focus on the nonequilibrium nature beyond biological details. By using a flexible coarse-grained polymer model and a spherical confinement, we find that confining and forcing the polymer chain to collapse along the nonequilibrium pathway makes the polymer to have less knotted conformations, of which relaxation toward an equilibrium globule is extremely slow.

II. MODEL AND METHOD

A. Simulation model and methods

We investigate the conformational transition of a single polymer chain immersed in an implicit solvent. The polymer is modeled as a bead-spring chain comprised of $N = 1024$ monomers of diameter σ , which is the unit length of this study. The nonbonding interaction between monomers is described by Week-Chandler-Andersen (WCA) potential [37]:

$$U_{\text{WCA}}(r) = \begin{cases} 4\epsilon\left[\left(\frac{\sigma}{r}\right)^{12} - \left(\frac{\sigma}{r}\right)^6\right] - \epsilon_{r_c}, & r < r_c \\ 0, & r \geq r_c \end{cases}$$

where $\epsilon = k_B T$ is the unit of energy. k_B and T denote the Boltzmann constant and temperature, respectively. The potential is truncated and shifted at a cutoff radius of $r_c = 1.122\sigma$ such that the potential is purely repulsive, where $\epsilon_{r_c} = 4\epsilon\left[\left(\frac{\sigma}{r_c}\right)^{12} - \left(\frac{\sigma}{r_c}\right)^6\right]$. The chemical bond between monomers is described by a harmonic potential, i.e., $U_b(r) = K(r - r_0)^2$ with $K = 1000k_B T \sigma^{-2}$ and $r_0 = \sigma$. The spatial confinement for the polymer chain is modeled as a sphere of radius R_{sph} . The wall of the sphere interacts with monomers via the same WCA potential but with r being the shortest distance between the monomer and the wall surface. In the condensation process of chromatin, the local charged interaction between DNA segments should play a critical role in generating a higher order chromatin structure in nature. The aim of this study is, however, not to mimic the condensation-decondensation

process of chromatin but to understand how the nonequilibrium nature of the transition pathway may affect the collapsed polymer conformation. As shall be discussed in Sec. III, without any specific interaction for the polymer chain, the polymer may form a fractal globule even under simple compression scheme.

We perform Langevin dynamics (LD) simulations via LAMMPS simulator [38] by solving the following equation of motion:

$$m \frac{d^2 r_i}{dt^2} = -\nabla_{r_i} U - \zeta \frac{dr_i}{dt} + F_i(t), \quad (1)$$

where r_i is the position vector of i th monomer. $F_i(t)$ denotes a random force exerted on the i th monomer at time t and satisfies the fluctuation-dissipation theorem, i.e., $\langle F_i(t) \rangle = 0$ and $\langle F_i(t) F_j(t') \rangle = 2\zeta k_B T \delta(t - t')$. The friction coefficient ζ is set to be 1. m is the mass of the monomers and is the unit of mass in this study. We use velocity-Verlet integrator and the integration time step is $\delta t = 0.005\tau$. τ is the reduced time unit, i.e., $\tau \equiv \sqrt{m\sigma^2/k_B T}$.

The volume fraction (ϕ) of the polymer chain inside a sphere is defined by $\phi = \frac{Nv_{\text{mon}}}{V}$, where $V = \frac{4}{3}\pi R_{\text{sph}}^3$ is the volume of the sphere and v_{mon} is the volume of a single monomer. We generate an initial configuration by adding monomers sequentially and growing a chain until it reaches a desired volume fraction. Then, we perform LD simulations for the initial configuration and equilibrate the system during at least the rotational relaxation time (τ_{rot}) of the end-to-end vector of the polymer, which is the longest relaxation mode of the chain. At a high volume fraction, the polymer chain of a large N would relax its conformation via reptation motions, which makes its conformational relaxation significantly slow. In order to accelerate the equilibration in chain conformations, we allow the polymer to undergo bond crossing temporarily by reducing a force constant K of the harmonic bonding potential (U_b) down to $K = 100k_B T \sigma^{-1}$ during equilibration runs. We confirm that a change in K from 1000 to 100 does not alter the overall chain conformations.

To investigate the polymer conformations, we calculate a segmental mean-squared distance [$R^2(s) \equiv \langle (r_i - r_j)^2 \rangle$] and a contact probability [$P(s)$] between two monomers i and j separated by $s = |i - j|$. When the distance $r = |r_i - r_j|$ is less than $a = 1.5\sigma$, two monomers are considered to make a contact. The contact probability is calculated by using $P(s) \equiv \frac{1}{N_{ij}} \sum_{i,j} \langle \theta(a - |r_i - r_j|) \rangle$. Here, N_{ij} is the total possible number of pairs of monomers separated by $|i - j|$. In order to investigate the conformational relaxation, we calculate a bond relaxation time (τ_b) and a rotational relaxation time (τ_{rot}). The time correlation functions of the bond vector are defined by $C_b(t) = \langle \frac{1}{2} [3(\frac{r_b(t)r_b(0)}{|r_b(t)||r_b(0)|})^2 - 1] \rangle$, where r_b is a bond vector of the polymer. The time correlation functions of an end-to-end vector are defined by $C_{ete}(t) = \langle \frac{r_{ete}(t)r_{ete}(0)}{|r_{ete}(t)||r_{ete}(0)|} \rangle$ where r_{ete} is the polymer end-to-end vector. τ_b and τ_{rot} are estimated using the relations $C_b(t = \tau_b) = e^{-1}$ and $C_{ete}(t = \tau_{\text{rot}}) = e^{-1}$.

B. Polymer collapse and knot formation

We investigate the confinement-induced polymer collapse, i.e., the conformational transition of the polymer chain from a coil to a globule, by changing the radius (R_{sph}) of the spherical

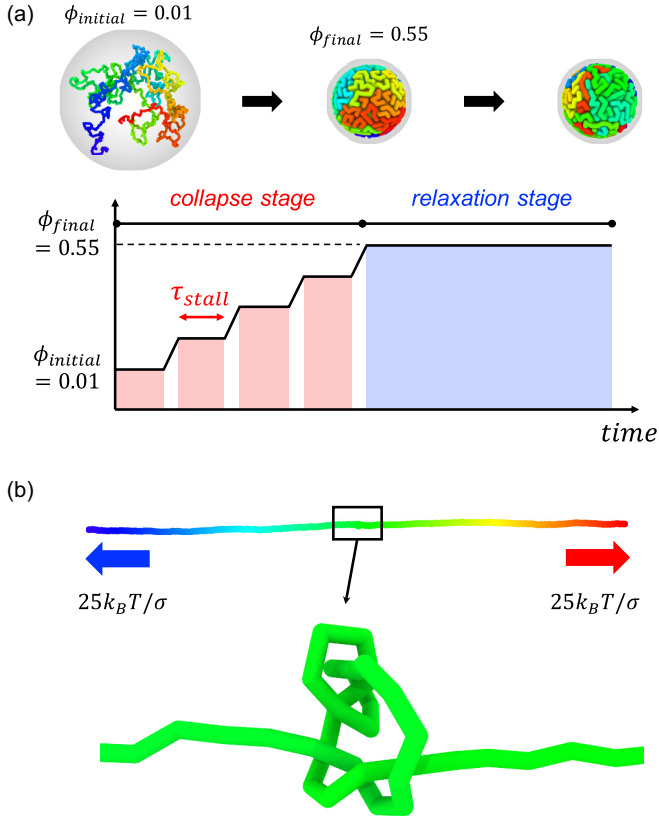


FIG. 1. (a) A simulation scheme for a collapse stage and a relaxation stage. (b) A pulling process where the two ends of the polymer is pulled to opposite directions with a constant force $25k_B T$. In the middle of the chain, a knotted region appears.

confinement. We change R_{sph} in a way that ϕ increases linearly with time from $\phi = 0.01$ to 0.55 . The collapse scheme consists of two stages as depicted in Fig. 1(a). In the first stage (*collapse stage*), we increase ϕ with a given rate of $d\phi/dt = 0.01$ by decreasing R_{sph} such that the polymer is forced to collapse. In order to tune the rate of the collapse, we insert a stalling step (of which duration is τ_{stall}) every time ϕ increases by 0.05 . Then, the polymer chain is allowed to relax its conformations during τ_{stall} . In case of $\tau_{\text{stall}} = 0$, the total time (τ_{collapse}) taken for the polymer chain to collapse is order of 10^1 , which is much smaller than $\tau_{\text{rot}} \approx O(10^3)$. Therefore, the longer τ_{stall} is, the polymer collapse is more likely to follow its reversible pathway as the polymer chain may retain its equilibrium conformations on the way to a globule. In this study, τ_{stall} ranges from 0 to $10\tau_{\text{rot}}$, where τ_{rot} varies depending on the current value of ϕ . In the second stage (*relaxation stage*), we let the polymer chain relax its conformation [Fig. 1(a)]. When the first collapse stage is completed, the last configuration of the chain is taken as a new initial configuration for the second relaxation stage. Then, we perform LD simulations with a fixed volume fraction of $\phi = \phi_{\text{final}} = 0.55$.

A polymer chain can be knotted and self-entangled inside a globule. In order to identify knots, we employ a pulling scheme by following the previous studies [39,40] [Fig. 1(b)]. In this scheme, we remove the wall potential and then we pull the polymer ends to opposite directions with a constant

force $25k_B T/\sigma$ until the polymer is fully stretched. If there were to be a knot in the polymer chain, the knotted region would appear in the middle of the stretched chain. The size of a knot (n_{knot}) is defined as the number of monomers that participate in the knot formation. We decide whether the i th monomer would belong to the knot as follows. For the i th monomer, we calculate a displacement vector (d_i) between two monomers ($i-1$) and ($i+1$) along the pulling force (y axis in our simulation), i.e., $d_i = [r_y(i+1) - r_y(i-1)]/2$. Here, $r_y(i)$ is the y component of the position vector of the i th monomer. When a monomer does not belong to the knot and is located outside the knotted region, $d_i \approx 1\sigma$ because the polymer is strongly stretched due to the pulling force. Otherwise, inside the knotted region, d_i decreases down to -0.5 . Then, we decide the i th monomer to participate in forming the knot when $d_i \leq 0.7$. We consider 1000 independent configurations from different initial configurations and calculate the probability (p_{knot}) of the knot being formed by dividing the number of configurations with any knots by the number of total configurations. For example, if 100 chains out of 1000 polymer chains would have knots, $p_{\text{knot}} = 0.1$.

III. DATA AND RESULTS

A. Conformation and its relaxation dynamics in equilibrium

In this section, we investigate the relaxation dynamics and the conformation of a polymer chain in a spherical confinement in an equilibrium state. Information on the relaxation dynamics and the conformation in equilibrium states allows us to compare to those in nonequilibrium states and understand how the (irreversible) transition pathway would affect the polymer conformation. In order to ensure that we obtain the equilibrium conformation inside a sphere, we generate a single polymer chain inside the sphere by allowing bond crossing and performing a random-walk generation process (i.e., growing the chain by adding monomers sequentially to the chain). Then, we perform additional LD simulations to equilibrate the polymer chain.

The conformation of the single polymer chain obtained from the above scheme is consistent with those expected for equilibrium states. Figures 2(b) and 2(c) depict the mean-squared spatial distance [$R^2(s)$] and the contact probability [$P(s)$] between two monomers i and j separated by $s = |i-j|$ along the chain. Both $R^2(s)$ and $P(s)$ are supposed to show scaling behaviors at small $s \leq N^{2/3}$ (before a monomer encounters the sphere boundary on average) [41] such that $R^2(s) \sim s^\alpha$ and $P(s) \sim s^{-\beta}$. For polymer chains in equilibrium, α is nearly equivalent to the flory exponent ν such that $\alpha = 2\nu$. $\nu = \frac{3}{5}$, $\frac{1}{2}$, and $\frac{1}{3}$ in good, theta, and poor solvent conditions, respectively [14]. In case of the contact probability $P(s)$, $P(s) \sim s^{-\beta}$ with $\beta = \frac{3}{2}$ for equilibrium globules [42] and $\beta \approx 2.18$ for unconfined self-avoiding walk chain [21]. The investigation of the values of β allows us to determine whether the transition to an equilibrium globule occurs or not.

$R^2(s)$'s are depicted for different values of ϕ in Fig. 2(b). Dotted lines are guides for the scaling relation with $\alpha = \frac{6}{5}$ and 1 for self-avoiding walk chains and globules, respectively. When $\phi = 0.01$, the single polymer chain is hardly perturbed by the spherical confinement and follows $R^2(s) \sim s^{6/5}$ like a

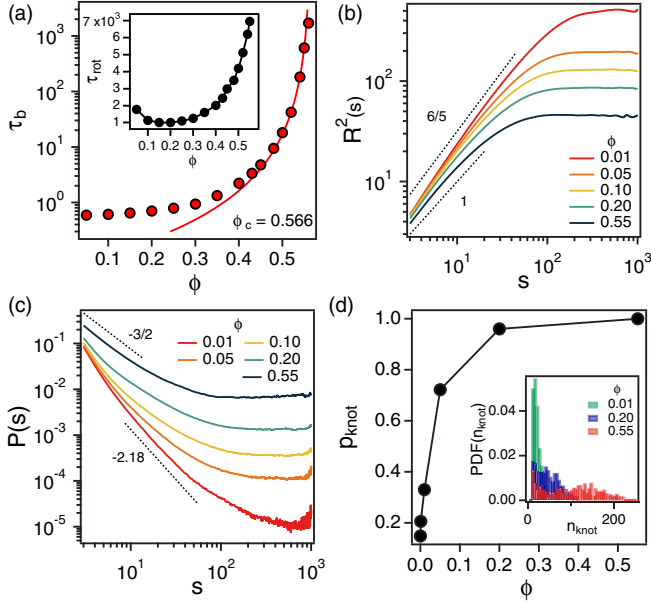


FIG. 2. (a) A bond relaxation time (τ_b) is plotted as a function of ϕ . The red solid line is a fitting line, $\tau_b \sim (\phi_c - \phi)^\gamma$ with $\phi_c = 0.566 \pm 0.002$ and $\gamma = 2.51 \pm 0.07$. (Inset) A rotational relaxation time (τ_{rot}) is plotted as a function of ϕ . (b) The mean-squared spatial distance [$R^2(s)$] between monomers i and j is plotted as a function of a distance $s = |i - j|$ for different ϕ . Dotted lines are guides for $R^2(s) \sim s^\alpha$ with $\alpha = \frac{6}{5}$ and 1. (c) The contact probability [$P(s)$] as a function of $s = |i - j|$ for different values of ϕ . Dotted lines are guides for $P(s) \sim s^\beta$ with $\beta = -\frac{2}{3}$ and -2.18 . (d) The knot probability (p_{knot}) as a function of ϕ . (Inset) Probability distribution function of n_{knot} for $\phi = 0.01, 0.2$, and 0.55 .

self-avoiding walk chain. As ϕ increases, the value of s at which $R^2(s)$ begins to level off shifts to a smaller value and the slope becomes lower due to a stronger confinement effect. When ϕ reaches 0.55 , $R^2(s) \sim s^1$ indicating that the polymer conformation is similar to that of an ideal chain, which is expected for an equilibrium polymer globule.

Figure 2(c) depicts the contact probability [$P(s)$] of the equilibrium polymer conformations for different values of ϕ . The exponent (β) changes from 2.18 to $\frac{3}{2}$ as ϕ increases from 0.01 to 0.55 . Note that $\beta = 2.18$ and $\frac{3}{2}$ correspond to those of the equilibrium self-avoiding chain and equilibrium globules, respectively. This indicates that we can obtain equilibrium conformations for different values of ϕ from 0.01 to 0.55 in this study.

Figure 2(a) depicts the bond relaxation time (τ_b) and the rotational relaxation time (τ_{rot}) for an equilibrium polymer chain under confinement. In general, τ_b and τ_{rot} represent the shortest and the longest p -mode relaxations of the polymer chain, i.e., the relaxation of polymer segments comprised of N/p monomers. As shown in Fig. 2(a), τ_b increases monotonically as ϕ is increased. A moderate increase in τ_b at low ϕ would result from an increase in local density inside a sphere. However, it begins to increase rapidly after $\phi \approx 0.25$. Kang *et al.* reported that the polymer chain showed glassy dynamics under strong confinement [21], which means that the polymer conformation would be dynamically arrested. At high ϕ , τ_b diverges and it is well fitted with a power-law

relation, i.e., $\tau_b \sim (\phi_c - \phi)^{-\gamma}$ as in supercooled liquids [43]. We extract from our simulations that $\phi_c \approx 0.566 \pm 0.002$ and $\gamma = 2.51 \pm 0.07$.

τ_{rot} shows a nonmonotonous behavior with respect to ϕ . At small $\phi \leq 0.2$, τ_{rot} slightly decreases as ϕ increases, which means the rotational relaxation is facilitated. In case of bulk polymer solutions, if Rouse scaling relation were to hold, $\tau_{\text{rot}} \sim \tau_b N^2 \approx 10^5$ to 10^6 . We find from simulations that for a polymer chain in bulk solution, $\tau_{\text{rot}} \approx 2 \times 10^5$. As shown in the inset of Fig. 2(a), however, τ_{rot} is relatively small for the polymer chain confined in the sphere. Even for the weakly confined chain of $\phi = 0.01$, the polymer chain certainly feels the boundary of the sphere, especially while the longest relaxation mode of the end-to-end vector relaxes. The collision of the polymer chain with the confinement wall may facilitate the relaxation of the longest relaxational motion, thus leading to a small value of τ_{rot} .

The polymer chain in the strong confinement is likely to form a knot. After equilibration, we employ the pulling scheme by removing the wall potential and pulling two ends with opposite directions [as in Fig. 1(b)]. Figure 2(d) depicts the knot probability (p_{knot}) as a function of ϕ . As shown in Fig. 2(d), the probability of forming a knot increases as ϕ increases. Even in a dilute bulk polymer solution ($\phi = 0$), $p_{\text{knot}} \approx 0.15$. Not surprisingly, p_{knot} depends on the degree of polymerization (N). The polymer chain of $N = 1024$ in our simulations is sufficiently long to form a knot without any confinement. When $\phi \geq 0.2$, p_{knot} reaches almost unity such that the polymer chain confined in a sphere with $\phi \geq 0.2$ almost always forms a knot. The probability distribution function (PDF) of n_{knot} is shown in the inset of Fig. 2(d). The size (n_{knot}) of a knot increases with an increase in ϕ . More interesting is that the complexity of knots (or the variation in n_{knot}) increases significantly with an increase in ϕ . For $\phi = 0.55$, the average knot size is about 100 ± 64 . A large standard deviation in n_{knot} implies that the knot conformations are diverse and heterogeneous.

B. Effects of the transition pathway on the chain conformation

We decrease the size (R_{sphere}) of the spherical confinement and increase the extent of the confinement for the polymer chain [Fig. 1(a)]. The polymer volume fraction (ϕ) inside the sphere increases gradually from $\phi = 0.01$ to 0.55 . The initial volume fraction of $\phi = 0.01$ is close to the overlap volume fraction of a bulk polymer, i.e., $\phi^* = N v_{\text{mon}} / \frac{4}{3} \pi R_g^3 \approx 0.005$ such that the confinement would not perturb the polymer conformation significantly at $\phi = 0.01$. The stalling time (τ_{stall}) ranges from 0 to $10\tau_{\text{rot}}$ in this simulation. Note that the value of τ_{rot} keeps changing depending on the current value of ϕ during the collapse process. In the relaxation stage, time (t) is reset and t denotes the elapsed time after the end of the collapse stage. We express time t by employing the value of τ_{rot} at $\phi = 0.55$.

Figures 3(a) and 3(b) depict how the contact probability [$P(s; t)$] and the mean-squared spatial distance [$R^2(s; t)$] change with t after the collapse stage. Black solid lines in Figs. 3(a) and 3(b) correspond to the equilibrium values of $P(s)$ and $R^2(s)$ at $\phi = 0.55$ [i.e., the same as in Figs. 2(b) and 2(c)]. We plot $P(s; t)$ and $R^2(s; t)$ for two extreme cases

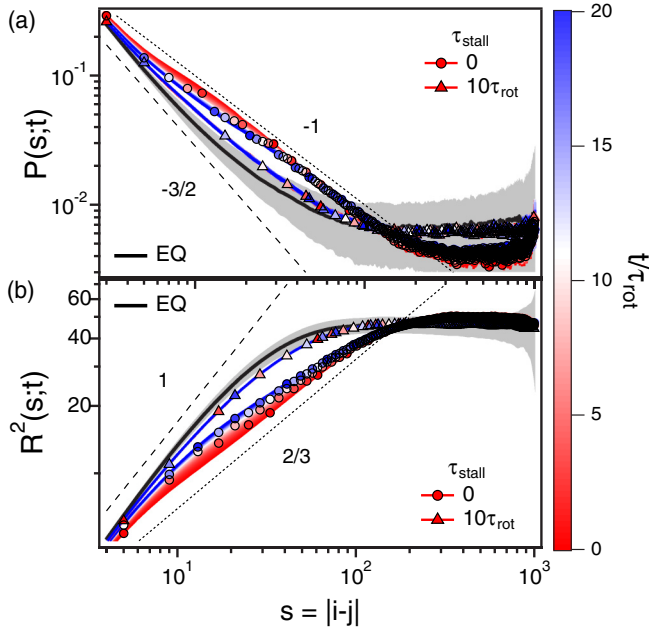


FIG. 3. (a) The contact probability $P(s;t)$ and (b) the mean-squared spatial distance $R^2(s;t)$ as a function of time t for $\tau_{\text{stall}} = 0$ and $10\tau_{\text{rot}}$. The elapsed time (t) after the collapse stage ranges from 0 to $20\tau_{\text{rot}}$. Dotted lines are guides for $P(s) \sim s^\beta$ and $R^2(s) \sim s^\alpha$.

of $\tau_{\text{stall}} = 0$ and $\tau_{\text{stall}} = 10\tau_{\text{rot}}$. Note that different symbols represent the different values of τ_{stall} and the different colors represent different times t .

In case of a fast collapse with $\tau_{\text{stall}} = 0$ (circles), the polymer chain is not allowed a sufficient amount of time to relax its conformation. The contact probability [$P(s;t=0)$, red circles] right after the collapse ($t=0$) deviates significantly from the equilibrium contact probability (black solid line). As time progresses in the relaxation stage, $P(s;t)$ changes slightly toward the equilibrium contact probability but is still far away from the equilibrium contact probability even at $t = 20\tau_{\text{rot}}$. In equilibrium, a leveling off in $P(s)$ occurs at $s \approx 100$ (black solid line), which corresponds to the theoretical value of $s \sim 1024^{2/3}$ where both $P(s)$ and $R^2(s)$ level off. This indicates that two monomers of $s \geq 100$ evenly contact with each other. On the other hands, $P(s;t)$'s of $\tau_{\text{stall}} = 0$ (red circles) level off at a much larger value of $s \approx 300$, which resembles the structure of the fractal globule. A perfect fractal globule would have a self-similar structure at all length scales and would not show any leveling off. The exponent β is close to -1 (for a fractal globule) rather than $-\frac{3}{2}$ (for an equilibrium globule) at medium s ranges. This indicates that the polymer chain obtained from a fast collapse transition has a similar structure with the fractal globule. More interesting is that $P(s;t)$ never fully relaxes into equilibrium even after $20\tau_{\text{rot}}$. After $t \geq 10\tau_{\text{rot}}$, $P(s;t)$ hardly changes with time, which means the polymer conformation is trapped in nonequilibrium states.

After the collapse transition, we allow the single polymer chain to relax its conformation for a long time until $t = 20\tau_{\text{rot}}$. We find, however, applying such a sufficiently long relaxation time (in the relaxation stage) does not guarantee that the polymer chain forms an equilibrium globule under the strong

confinement. In case of $\tau_{\text{stall}} = 10\tau_{\text{rot}}$ [triangles in Fig. 3(a)], where the rotational motion of the polymer would be fully relaxed during the collapse stage, $P(s;t)$ hardly changes with time. This indicates that the polymer conformation reaches a steady state. However, there is still a non-negligible deviation from the equilibrium $P(s)$ (black solid line).

Similar trends are observed in $R^2(s;t)$ as shown in Fig. 3(b). In equilibrium simulations, $R^2(s)$ scales as $R^2(s) \sim s^1$, which is consistent with what is expected for a random-walk chain in polymer melts. In case of the polymer chain after the collapse transition, $R^2(s;t)$ deviates from its equilibrium counterpart regardless of the magnitude of τ_{stall} . At $t = 0$ after the collapse transition, $R^2(s;t) \sim s^{2/3}$, which is expected for a polymer globule in poor solvent. Since the fractal globule is constructed by iterative collapses of local globules, the scaling relation of the size of polymer segments of s monomers, $R(s) \sim s^{1/3}$, is consistent with the scaling relation of the entire polymer chain of N monomers, i.e., $R(N) \sim N^{1/3}$. Leveling off also appears at a later time for the polymer chain after the collapse transition than in equilibrium simulations.

Previous studies investigated the conformation of a confined polymer as a model for chromatin organization. Kang *et al.* [21] reported that the glassy dynamics of the polymer chain under strong spherical confinement could be the reason of a nonequilibrium chromatin organization. In order to obtain the conformations of a confined polymer, they chose to reduce the size of the spherical confinement with a finite compression rate. On the other hands, Gürsoy *et al.* [7] suggested an algorithm that could generate a large number of ensembles of a model chromatin fiber in severe spatial confinements, which was called a constrained self-avoiding chromatin (C-SAC) model. They reported that the available free volume would be a key determinant for chromosome folding and its architecture. According to our simulations, the polymer conformation [characterized by both $P(s;t)$ and $R^2(s;t)$] may differ depending on how the polymer chain conformation is generated, especially whether the polymer chain is located and equilibrated within a confinement or the polymer chain is compressed with a various compression rate (or τ_{stall}).

Regardless of the magnitude of τ_{stall} , $P(s;t)$ converges into a steady state at long times, at least within our simulation times. Figures 4(a) and 4(b) depict $P(s;t = 20\tau_{\text{rot}})$ and $R^2(s;t = 20\tau_{\text{rot}})$ at a long time $t = 20\tau_{\text{rot}}$ for different values of τ_{stall} . The different values of τ_{stall} mean that the polymer chain is allowed to relax its conformation for different duration in the collapse transition. Both $P(s;t = 20\tau_{\text{rot}})$ and $R^2(s;t = 20\tau_{\text{rot}})$ (which correspond to those of the steady state) differ for different values of τ_{stall} . This indicates that the polymer chain conformation [$P(s;t)$ and $R^2(s;t)$] in the steady state should depend on the transition rate (and pathway), which is the signature of nonequilibrium nature.

$P(s)$ was measured experimentally by chromosome capture techniques such as genome-wide 3C (Hi-C). Conventional Hi-C methods measured chromosomal contacts averaged over a large ensemble of cells. However, it is still challenging to interpret the ensemble-averaged Hi-C data and predict the three-dimensional organization of chromatin by developing a universal model [5,6,11,15,20,44,45], due to a significant cell-to-cell variability even in isogenic cell lines, especially

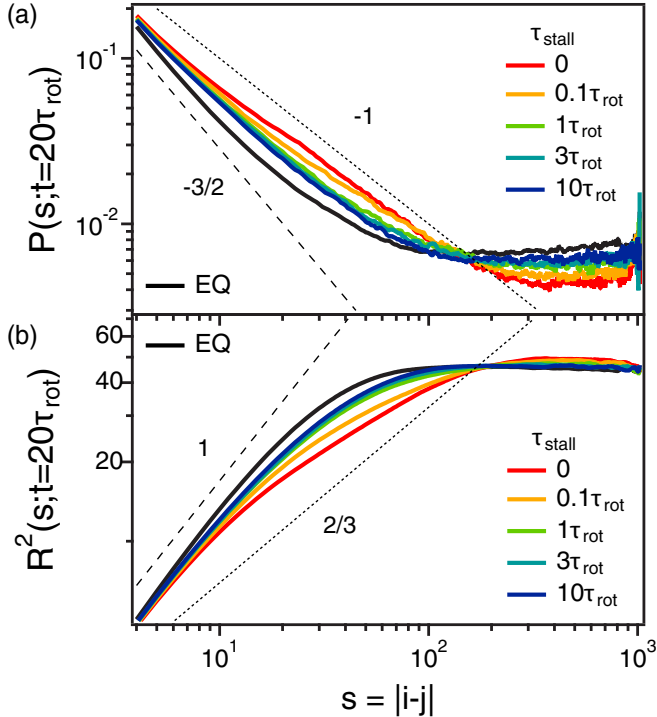


FIG. 4. (a) The contact probability $P(s; t = 20\tau_{\text{rot}})$ and (b) the mean-squared spatial distance $R^2(s; t = 20\tau_{\text{rot}})$ at $t = 20\tau_{\text{rot}}$ for different values of τ_{stall} . Dotted lines are guides for $P(s) \sim s^\beta$ and $R^2(s) \sim s^\alpha$. Numbers indicate exponents α and β .

for long-range contacts [13,46]. Stochastic and heterogeneous scalings of chromatin contacts could be understood in the context of the nonequilibrium nature of biological systems. The conformations of a confined or collapsed polymer chain could not relax fully into a conformation at a free-energy minimum, but might remain in nonequilibrium states with diverse conformations. Our data also suggest that the contact probability [$P(s)$] is highly sensitive to spatial confinement and how the polymer collapse transition occurs, which could be a reason for the heterogeneity of the exponent α observed in experiments.

C. Effects of the transition pathway on the knot formation

Fractal globules are known to have knot-free conformations [41]. If a chromatin were to form a fractal globule, it would enable densely packed chromatin to fold and unfold any genomic loci easily without topological hindrance. How and whether the confined chromatin has knot-free conformations are, therefore, of biological importance, but still remain unclear. We find from our simulations that a fast collapse transition of a polymer chain can induce less knotted conformations. Figure 5(a) depicts the probability (p_{knot}) of finding knots in a polymer chain. We calculate p_{knot} at two different moments: (1) at $t = 0$ right after the collapse transition is completed and (2) at $t = 20\tau_{\text{rot}}$ long after the collapse transition. Note that when the polymer chain is equilibrated in our equilibrium simulations for $\phi = 0.55$, $p_{\text{knot}} \approx 1$. In other words, a polymer chain in equilibrium almost always forms a knot within a strong confinement.

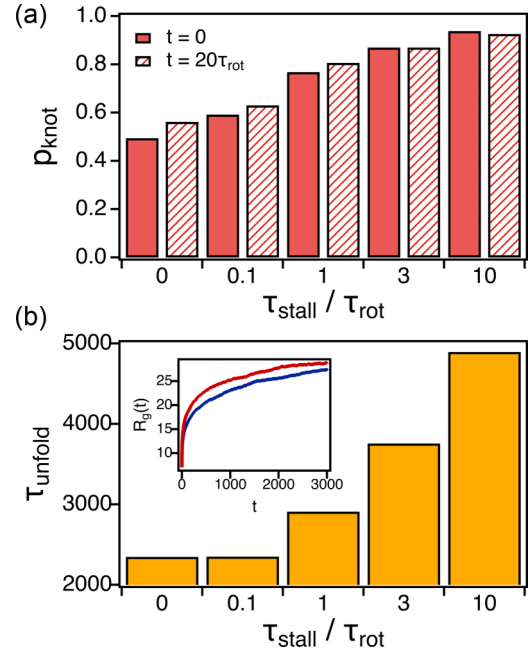


FIG. 5. (a) The knot probability (p_{knot}) for different stalling times $\tau_{\text{stall}} = 0, 0.1\tau_{\text{rot}}, \tau_{\text{rot}}, 3\tau_{\text{rot}},$ and $10\tau_{\text{rot}}$. Solid bars represent p_{knot} estimated at $t = 0$ and hatched bars represent p_{knot} at $t = 20\tau_{\text{rot}}$. (b) The unfolding time (τ_{unfold}) as a function of τ_{stall} . (Inset) The radius of gyration (R_g) as a function of time t for $\tau_{\text{stall}} = 0$ (red) and $10\tau_{\text{rot}}$ (blue). R_g is averaged over 1000 different initial configurations.

As shown in Fig. 5(a), p_{knot} ranges from 0.5 to 0.93 and depends on the stalling time (τ_{stall}). p_{knot} increases with an increase in τ_{stall} . Compared to the equilibrium value of $p_{\text{knot}} \approx 1$ at $\phi = 0.55$, the formation of knots is inhibited effectively by up to 50% depending on the collapse rate. Even if we let the polymer chain to relax during $20\tau_{\text{rot}}$ after the collapse transition, p_{knot} hardly changes, which means that the knot probability is determined mostly during the collapse transition. Once the collapse transition is complete, a new knot hardly forms even at long times. However, if we allow the polymer chain to relax its conformation for a longer duration (τ_{stall}) along the collapse transition, the polymer chain is more likely to form a knot inside the sphere.

The extent of the knot formation also affects the unfolding rate of the polymer chain. We estimate an unfolding time (τ_{unfold}) by measuring the time for a collapsed polymer to swell when the spherical confinement is removed. We perform LD simulations by using the conformation at $t = 0$ right after the collapse transition as a new initial configuration and removing the spherical wall potential. In the absence of the confinement, the polymer chain unfolds spontaneously due to a high pressure built during the collapse process. By monitoring the radius of gyration [$R_g(t)$] of the polymer as a function of time, we define τ_{unfold} by using the relation $R_g(t = \tau_{\text{unfold}}) = 0.7R_{g,\text{bulk}}$. Here, $R_{g,\text{bulk}} = 29.6$ is the ensemble-averaged equilibrium value of the polymer chain in bulk solutions. As depicted in Fig. 5(b), τ_{unfold} increases with an increase in τ_{stall} . τ_{unfold} is almost doubled when $\tau_{\text{stall}} = 10\tau_{\text{rot}}$ compared to the fastest collapse transition. As we allow the polymer chain to relax its conformation, the

chain conformations become complex with more knots such that it takes more time for the polymer chain to unfold and recover its bulk conformations. We also estimate the position of the end monomers and its distribution functions during the unfolding process. We find that in case of the fastest collapse of $\tau_{\text{stall}} = 0$, the end monomers of the polymer chain are likely to be placed at the boundary of the polymer globule. On the other hand, for the slow collapse of $\tau_{\text{stall}} = 10\tau_{\text{rot}}$, the end monomers are more likely to be placed inside the globule such that the unfolding becomes slower.

IV. CONCLUSION

We perform two different sets of LD simulations for a single polymer chain confined within a sphere. In the first set of LD simulations, we place the polymer chain within a fixed radius (R_{sph}) of the sphere (and hence the volume fraction ϕ is fixed). But, we reduce the bonding potential parameter (K) such that the polymer undergoes extensive bond-crossing events and the polymer chain obtains equilibrium conformations. Then, we increase the value of K back to $K = 1000k_B T \sigma^{-2}$ and propagate the system via LD simulations. In the second set of LD simulations, we place a single polymer chain within a relatively large sphere (with $\phi = \phi_{\text{initial}} = 0.01$) and then reduce the value of R_{sph} gradually, which we call the collapse stage. Within the collapse stage, we sometimes stop collapsing the sphere and the chain, and let the polymer chain to relax its conformation during the time τ_{stall} . We change the value of τ_{stall} and investigate its effect on the collapsed conformation. After ϕ reaches $\phi_{\text{final}} = 0.55$, we complete the collapse transition, reset the time t , and perform LD simulations, which we call the relaxation stage. We compare the conformations from both sets of LD simulations in order to investigate the effect of the transition pathway on the chain conformations.

The conformations obtained from the first set of LD simulations are close to those of equilibrium globules. The contact probability [$P(s)$] scales as $P(s) \sim s^{-3/2}$ for $s < 10^2$ for $\phi = 0.55$, which is expected for the equilibrium globules. Similarly, the mean-squared spatial distance [$R^2(s)$] scales as

$R^2(s) \sim s^1$, which indicates that the polymer chain behaves as an ideal chain globule inside the confinement.

On the other hand, when the polymer chain is forced to collapse along the irreversible pathway, the polymer conformation [characterized by $P(s)$ and $R^2(s)$] stays away from equilibrium conformations. And $P(s)$ and $R^2(s)$ depend on how fast the collapse of the chain occurs. More interestingly, the polymer conformation becomes similar to the fractal globule such that $P(s)$ scales as $P(s) \sim s^{-1}$. This indicates that the fast irreversible transition may lead to nonequilibrium polymer conformation inside the confinement. When a polymer chain collapses quite fast with $\tau_{\text{stall}} = 0$, the polymer chain would not have a sufficient amount of time to relax its conformation during the collapse. Once the collapse transition is complete and ϕ reaches $\phi_{\text{final}} = 0.55$, the relaxation of the nonequilibrium conformations from the fast transition hardly occurs due to slow dynamics.

The knot formation also depends on the collapse transition pathway. Compared to equilibrium conformations with many knots, the polymer globule generated by the collapse transition exhibits fractal globulelike and less knotted conformations. Without any specific interactions between monomers, the knot formation is inhibited effectively in a fast collapsed polymer globule. We also show that less knotted polymer globule unfolds easily when the spatial confinement disappears.

ACKNOWLEDGMENTS

This work was supported by Samsung Science and Technology Foundation under Project No. SSTF-BA1502-07. This research was supported by the Basic Science Research Program through the National Research Foundation of Korea (NRF) funded by the Ministry of Education (Grant No. 2018R1A6A1A03024940). This research was also supported by the Creative Materials Discovery Program (Grant No. 2018M3D1A1057844) through the NRF funded by the Ministry of Science and ICT. This work was supported by the National Research Foundation of Korea (NRF) grant funded by the Korea government (MSIT) (Grant No. 2019R1A2C2084053).

-
- [1] N. Gilbert, S. Boyle, H. Fiegler, K. Woodfine, N. P. Carter, and W. A. Bickmore, *Cell* **118**, 555 (2004).
 - [2] A. Wolffe, *Chromatin: Structure and Function* (Academic, New York, 1998).
 - [3] E. Lieberman-Aiden, N. L. van Berkum, L. Williams, M. Imakaev, T. Ragozcy, A. Telling, I. Amit, B. R. Lajoie, P. J. Sabo, M. O. Dorschner, R. Sandstrom, B. Bernstein, M. A. Bender, M. Groudine, A. Gnirke, J. Stamatoyannopoulos, L. A. Mirny, E. S. Lander, and J. Dekker, *Science* **326**, 289 (2009).
 - [4] K. van Holde and J. Zlatanova, *Semin. Cell Dev. Biol.* **18**, 651 (2007).
 - [5] B. Zhang and P. G. Wolynes, *Proc. Natl. Acad. Sci. USA* **112**, 6062 (2015).
 - [6] J. Mateos-Langerak, M. Bohn, W. de Leeuw, O. Giromus, E. M. M. Manders, P. J. Verschure, M. H. G. Indemans, H. J. Gierman, D. W. Heermann, R. van Driel, and S. Goetze, *Proc. Natl. Acad. Sci. USA* **106**, 3812 (2009).
 - [7] G. Gürsoy, Y. Xu, A. L. Kenter, and J. Liang, *Nucleic Acids Res.* **42**, 8223 (2014).
 - [8] R. Wang, J. Mozziconacci, A. Bancaud, and O. Gadal, *Curr. Opin. Cell Biol.* **34**, 54 (2015).
 - [9] M. Barbieri, M. Chotalia, J. Fraser, L.-M. Lavitas, J. Dostie, A. Pombo, and M. Nicodemi, *Proc. Natl. Acad. Sci. USA* **109**, 16173 (2012).
 - [10] M. Tark-Dame, R. van Driel, and D. W. Heermann, *J. Cell Sci.* **124**, 839 (2011).
 - [11] M. Barbieri, A. Scialdone, and A. Piccolo, *Front. Genet.* **4**, 113 (2013).
 - [12] J. Dekker, K. Rippe, M. Dekker, and N. Kleckner, *Science* **295**, 1306 (2002).

- [13] T. Nagano, Y. Lubling, T. J. Stevens, S. Schoenfelder, E. Yaffe, W. Dean, E. D. Laue, A. Tanay, and P. Fraser, *Nature (London)* **502**, 59 (2013).
- [14] M. Rubinstein and R. H. Colby, *Polymer Physics* (Oxford University Press, Oxford, 2003).
- [15] A. Grosberg, Y. Rabin, and S. Havlin, *Europhys. Lett.* **23**, 373 (1993).
- [16] T. Sexton, E. Yaffe, E. Kenigsberg, F. Bantignies, B. Leblanc, M. Hoichman, H. Parrinello, A. Tanay, and G. Cavalli, *Cell* **148**, 458 (2012).
- [17] R. Kalhor, H. Tjong, N. Jayathilaka, F. Alber, and L. Chen, *Nat. Biotechnol.* **30**, 90 (2011).
- [18] H. Albiez, M. Cremer, C. Tiberi, L. Vecchio, L. Schermelleh, S. Dittrich, K. Küpper, B. Joffe, T. Thormeyer, J. von Hase, S. Yang, K. Rohr, H. Leonhardt, I. Solovei, C. Cremer, S. Fakan, and T. Cremer, *Chromosome Res.* **14**, 707 (2006).
- [19] K. J. Meaburn and T. Misteli, *Nature (London)* **445**, 379 (2007).
- [20] M. Bohn and D. W. Heermann, *PLoS ONE* **5**, e12218 (2010).
- [21] H. Kang, Y.-G. Yoon, D. Thirumalai, and C. Hyeon, *Phys. Rev. Lett.* **115**, 198102 (2015).
- [22] X. Hu, L. Hong, M. Dean Smith, T. Neusius, X. Cheng, and J. C. Smith, *Nat. Phys.* **12**, 171 (2015).
- [23] H. Qian and T. C. Reluga, *Phys. Rev. Lett.* **94**, 028101 (2005).
- [24] W. Min, X. S. Xie, and B. Bagchi, *J. Chem. Phys.* **131**, 065104 (2009).
- [25] R. Metzler, J. H. Jeon, and A. G. Cherstvy, *Biochim. Biophys. Acta: Biomembranes* **1858**, 2451 (2016).
- [26] D. E. Piephoff, J. Wu, and J. Cao, *J. Phys. Chem. Lett.* **8**, 3619 (2017).
- [27] E. M. Popov, *Biochem. Mol. Biol. Int.* **47**, 443 (1999).
- [28] Z. T. Berendsen, N. Keller, S. Grimes, P. J. Jardine, and D. E. Smith, *Proc. Natl. Acad. Sci. USA* **111**, 8345 (2014).
- [29] Y. R. Chemla and T. Ha, *Science* **345**, 380 (2014).
- [30] S. Kwon, S. Lee, H. W. Cho, J. Kim, J. S. Kim, and B. J. Sung, *J. Chem. Phys.* **150**, 204901 (2019).
- [31] S. Kwon and B. J. Sung, *Phys. Rev. E* **100**, 042501 (2019).
- [32] S. Kwon and B. J. Sung, *J. Chem. Phys.* **149**, 244907 (2018).
- [33] S. Kwon, H. W. Cho, J. Kim, and B. J. Sung, *Phys. Rev. Lett.* **119**, 087801 (2017).
- [34] N. Keller, S. Grimes, P. J. Jardine, and D. E. Smith, *Nat. Phys.* **12**, 757 (2016).
- [35] R. N. Mukherjee, P. Chen, and D. L. Levy, *Nucleus* **7**, 167 (2016).
- [36] F.-Y. Chu, S. C. Haley, and A. Zidovska, *Proc. Natl. Acad. Sci. USA* **114**, 10338 (2017).
- [37] J. D. Weeks, D. Chandler, and H. C. Andersen, *J. Chem. Phys.* **54**, 5237 (1971).
- [38] S. Plimpton, *J. Comput. Phys.* **117**, 1 (1995).
- [39] L. Dai and P. S. Doyle, *Macromolecules* **51**, 6327 (2018).
- [40] C. B. Park, S. Kwon, and B. J. Sung, *J. Chem. Phys.* **151**, 054901 (2019).
- [41] L. A. Mirny, *Chromosome Res.* **19**, 37 (2011).
- [42] R. Lua, A. L. Borovinskiy, and A. Y. Grosberg, *Polymer* **45**, 717 (2004).
- [43] W. Kob and H. C. Andersen, *Phys. Rev. E* **52**, 4134 (1995).
- [44] H. Tjong, W. Li, R. Kalhor, C. Dai, S. Hao, K. Gong, Y. Zhou, H. Li, X. J. Zhou, M. A. Le Gros, C. A. Larabell, L. Chen, and F. Alber, *Proc. Natl. Acad. Sci. USA* **113**, E1663 (2016).
- [45] A. M. Chiariello, C. Annunziatella, S. Bianco, A. Esposito, and M. Nicodemi, *Sci. Rep.* **6**, 29775 (2016).
- [46] J. Kind, L. Pagie, H. Ortabozkoyun, S. Boyle, S. S. de Vries, H. Janssen, M. Amendola, L. D. Nolen, W. A. Bickmore, and B. van Steensel, *Cell* **153**, 178 (2013).